C$_{60}$ as a versatile electron contact material for crystalline silicon solar cells

Yuchen Sun[1], Jesus Ibarra Michel[1], Daniela Bozanic[1], Pheng Phang[2], Heping Shen[2], Jie Yang[3], Peiting Zheng[2], Xinyu Zhang[3], Di Yan[1] and James Bullock[1]

[1]*The University of Melbourne, Parkville, Australia*
[2]*Australian National University, Canberra, Australia*
[3]*Jinko Solar Co., Ltd, Zhejiang, China*

yucsun1@student.unimelb.edu.au
james.bullock@unimelb.edu.au

Introduction

Passivating contacts are crucial in obtaining high efficiencies in crystalline silicon (c-Si) solar cells. Several materials are being used as passivating contacts to achieve high efficiencies (>23%), such as polysilicon (poly-Si), amorphous silicon (a-Si), titanium dioxide (TiO$_2$), and molybdenum trioxide (MoO$_3$).[1] [2] [9] Finding a material that either by itself or combined with other passivation layers allows for both good passivation and low specific contact resistivity ρ_c is still an active research area. The fullerenes, such as C$_{60}$, remain relatively unexplored as contact interlayers in c-Si solar cells[11], despite the fact they are routinely used as a thin interlayer (e.g. 20 nm) in other devices, such as organic light emitting diodes, organic solar cells, and perovskite solar cells.[10] This abstract explores the versatile behaviour of C$_{60}$ thin films when used either as an electron selective layer directly on c-Si, or as a protective layer in poly-Si/SiO$_2$ based electron passivating contacts.

For the direct application of C$_{60}$ as an electron selective layer for c-Si, we take advantage of the changes that C$_{60}$ experiences over time when exposed to air atmosphere, as also observed by other research groups.[4] [8] In our observations, these changes led to an improvement in ρ_c over time, as opposed to other materials which degrade over time. Following that, we show that C$_{60}$ can also serve as a protective interlayer between an n$^+$poly-Si/SiO$_2$ contact stack and its metal electrode. This prevents interaction between the layers at moderate annealing temperatures (e.g., 500 °C) preserving the passivation quality of the poly-Si/SiO$_2$ contact. These two experiments highlight the promising prospects of integrating C$_{60}$ into conventional silicon photovoltaics.

Experiment

For the first part of this study, C$_{60}$ is used as an electron selective layer. Transfer length method (TLM) samples were prepared on ~1 Ω-cm n-type c-Si substrates. These TLM structures, shown in Figure 1a, were fabricated by first cleaning substrates in a dilute HF etch followed by thermally evaporating C$_{60}$ (2-10 nm) and Al (~200 nm) stacks through a shadow mask, at a base pressure < 10^{-6} mbar. Current-voltage (I-V) measurements were taken with a custom made 4-probe setup.

For the second part of the study, contact samples are made using the Cox and Strack (C&S) pattern. Initially, n$^+$poly-Si/SiO$_2$/c-Si(n)/SiO$_2$/n$^+$poly-Si substrates were made on n-type ~2 Ω-cm wafers, by first depositing full-area SiO$_2$ (1-2 nm) and phosphorus doped silicon (10 nm) films on both sides via low pressure chemical vapour deposition (LPCVD), and then annealing to activate the dopants. Following this, the front side of the samples were deposited with full-area C$_{60}$ (20-80 nm) films, followed by Al (~200 nm) dots deposited through a C&S shadow mask. The rear side of samples was deposited with a full-area Al layer. Current-voltage (I-V) measurements were taken with a custom 4-probe setup. An accompanying set of samples for photoluminescence (PL) imaging were made from identical n$^+$poly-Si/SiO$_2$/c-Si(n)/SiO$_2$/n$^+$poly-Si substrates. These samples had four regions with different film combinations deposited on the rear side: *i.* a C$_{60}$/Al region, *ii.* a C$_{60}$ region, *iii.* an Al region, and *iv.* a blank region. Photoluminescence measurements were taken using a

custom-built PL line scan camera. The samples were illuminated with a λ=808 nm laser and the PL response was measured using an InGaAs line scan camera filtered to remove the illumination wavelengths.

Key Results

Figure 1a illustrates the variation in ρ_c as a function of air exposure time for different thicknesses of C_{60} on n-type c-Si. The C_{60} thicknesses used were 2 nm, 5 nm, and 10 nm. For all three thicknesses, ρ_c starts with a relatively high value after deposition (around 1-10 $\Omega\,cm^2$), following which they undergo a consistent decrease over time reaching values below 0.2 $\Omega\,cm^2$. In other studies, it has been documented that C_{60} changes its characteristics when exposed to water vapor or oxygen in the air [4] [8]. To test the influence of the ambient, this study also explored the evolution of ρ_c vs. time when the samples are exposed to different environments. Figure 1b illustrates this by comparing two samples: one sample kept in nitrogen (except when measuring ρ_c, since the I-V setup is in air), and the other kept in ambient air. The sample kept in nitrogen shows a slight increase in ρ_c over time. The lower starting value may be caused by ambient air exposure during frequent IV measurements at the beginning. The sample kept in ambient air has a consistent decrease in ρ_c over time. This sample was moved into the nitrogen chamber after 12 days, shown as the dashed line in Figure 1b. After the environment changed, the ρ_c of the sample gradually increased, consistent with the behaviour of the other nitrogen-only sample. This comparison confirms the positive influence that air (most likely due to water or oxygen molecules) has on the ρ_c behaviour of the C_{60} layers.
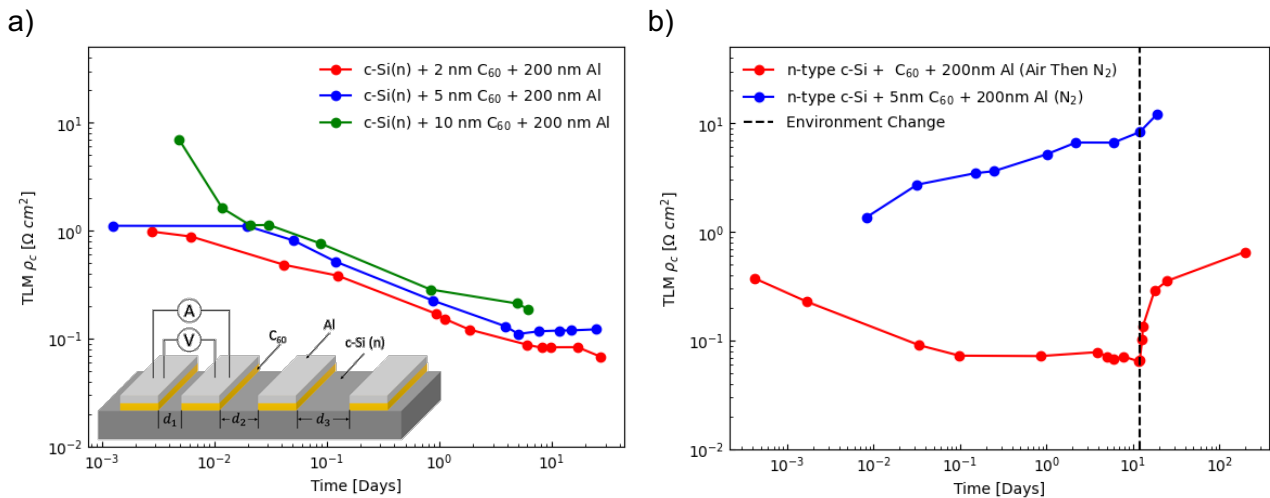
a)   b)

Figure 1. a) ρ_c of C_{60}/c-Si electron contacts as a function of time with different C_{60} thickness (2, 5 and 10 nm). The inset shows the TLM structure used to measure ρ_c. b) ρ_c of C_{60}/c-Si electron contacts as a function of time when stored in different environments (air and N_2). The dashed vertical line indicates when the sample was removed from air and instead stored in an N_2 ambient.

In the second application, we have assessed the usefulness of C_{60} as a protective interlayer between an Al electrode and a thin n^+poly-Si/SiO_2 passivating contact after an annealing step (up to 500°C). A very thin n^+poly-Si layer of ~10 nm, was chosen as an extreme case as it is known to be quite sensitive, in terms of passivation degradation, to an Al direct metallisation (for example, evaporated Al). These starting substrates had implied open circuit voltages iV_{oc} in the range of ~710 mV, as measured using the photoconductance decay method. To measure how effective C_{60} is in separating the poly-Si and Al layers, photoluminescence (PL) imaging is used as a proxy for the carrier lifetime

of the sample. As shown in Figure 2a, these samples had four regions with different film combinations deposited on the rear-side: a C_{60}/Al region (top left), a C_{60} region (bottom left), an Al region (top right), and a blank region (bottom right). It can be seen in all three samples that the regions with direct Al exhibited lower PL emission even in the as-deposited case, with almost no PL emission after annealing at 400°C, confirming the sensitivity of the thin poly-Si layer to damage from the Al layer. The addition of the C_{60} layer improves this, maintaining bright PL in the as-deposited case. Protection is seen at 400°C for the thicker (i.e., 80 nm) C_{60} films, with PL counts similar to the non-metallised regions. Some protection is even seen at 500°C, indicating the promise of this approach.

For the C_{60} layers to serve as protective coatings they should also not significantly compromise the ρ_c of the poly-Si passivating contact structures. Figure 2b provides a comparison of how the poly-Si contact stacks ρ_c varies with different thicknesses of C_{60} and annealing temperature. Although there is no clear trend or correlation between the temperature and thickness with ρ_c, the value of ρ_c is still low even after the addition of 80 nm of C_{60}, with and without annealing. This suggests C_{60} as a candidate for protecting against degradation when metallising poly-Si contacts. We did not measure any significant changes in ρ_c for the c-Si/SiO$_2$/n$^+$poly-Si/C$_{60}$/Al contacts over time when exposed to air, unlike results obtained in Figure 1 for c-Si(n)/C$_{60}$/Al contacts.
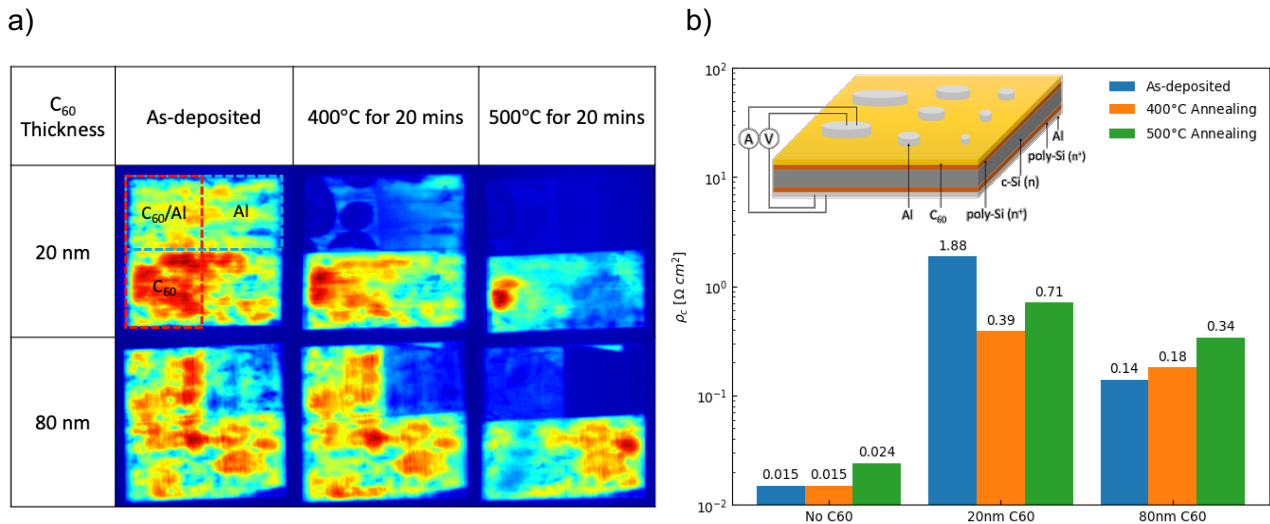
a)

b)

Figure 2. a) PL images of samples with C$_{60}$ (20, 80 nm) and Al (~200nm) thin films on top of poly-Si passivated electron contacts. b) ρ_c of SiO$_2$/n$^+$poly-Si/C$_{60}$/Al electron contacts as a function of annealing temperature with different C$_{60}$ thickness (20, 80 nm). Results for SiO$_2$/n$^+$poly-Si/Al electron contacts (i.e., without the C$_{60}$ layer) are included for reference. Inset shows the Cox and Strack method structure used to measure ρ_c.

Conclusion

In summary, investigation of the use of C_{60} in electron contacts for silicon solar cells shows two promising applications. This includes being used as a direct electron contact layer in n-type silicon, yielding ρ_c values of below 0.2 $\Omega\ cm^2$. Interestingly, these contacts show improved behaviour when subjected to air exposure. Another use of C_{60} is its ability to separate poly-Si layers from metal electrodes, preventing significant passivation degradation during annealing steps. In this application, it was found that C_{60} interlayers of 80 nm were sufficient to completely maintain the passivation (i.e., iV_{oc} ~ 710 mV) of metallised poly-Si contacts after annealing at 400°C for 20 minutes. Based on these results, C_{60} has potential for use in electron contacts for silicon solar cells, and further research should be done on this material.

References

[1] Yan, D., Cuevas, A., Michel, J. I., Zhang, C., Wan, Y., Zhang, X., & Bullock, J. (2021). Polysilicon passivated junctions: The next technology for silicon solar cells?. *Joule*, *5*(4), 811-828.

[2] Yan, D., Cuevas, A., Stuckelberger, J., Wang, E. C., Phang, S. P., Kho, T. C., ... & Bullock, J. (2023). Silicon solar cells with passivating contacts: Classification and performance. *Progress in Photovoltaics: Research and Applications*, *31*(4), 310-326.

[3] Schroder, D. K. (2015). *Semiconductor material and device characterization*. John Wiley & Sons.

[4] Ahmed, R., Simbrunner, C., Schwabegger, G., Baig, M. A., & Sitter, H. (2014). Air stability of C60 based n-type OFETs. *Synthetic metals*, *188*, 136-139.

[5] Chibante, L. F., & Heymann, D. (1993). On the geochemistry of fullerenes: stability of C60 in ambient air and the role of ozone. *Geochimica et cosmochimica acta*, *57*(8), 1879-1881.

[6] Haddon, R. C., Perel, A. S., Morris, R. C., Palstra, T. T. M., Hebard, A. F., & Fleming, R. M. (1995). C60 thin film transistors. *Applied physics letters*, *67*(1), 121-123.

[7] Jang, J., Kim, J. W., Park, N., & Kim, J. J. (2008). Air stable C60 based n-type organic field effect transistor using a perfluoropolymer insulator. *Organic electronics*, *9*(4), 481-486.

[8] Tapponnier, A., Biaggio, I., & Günter, P. (2005). Ultrapure C60 field-effect transistors and the effects of oxygen exposure. *Applied Physics Letters*, *86*(11).

[9] Bullock, J., Cuevas, A., Allen, T., & Battaglia, C. (2014). Molybdenum oxide MoOx: A versatile hole contact for silicon solar cells. *Applied Physics Letters*, *105*(23).

[10] Bao, C., Chen, C., Muhammad, M., Ma, X., Wang, Z., Liu, Y., ... & Duan, Y. (2019). Hybrid perovskite charge generation layer for highly efficient tandem organic light-emitting diodes. *Organic Electronics*, *73*, 299-303.

[11] Duan, L., Walter, D., Chang, N., Bullock, J., Kang, D., Phang, S. P., ... & Shen, H. (2023). Stability challenges for the commercialization of perovskite–silicon tandem solar cells. *Nature Reviews Materials*, *8*(4), 261-281.